



Cite this: *Phys. Chem. Chem. Phys.*,
2016, 18, 11480

Homonuclear decoupling for spectral simplification of carbon-13 enriched molecules in solution-state NMR enhanced by dissolution DNP†

Srinivas Chinthalapalli,^{ab} Aurélien Bornet,^a Diego Carnevale,^{*ac} Sami Jannin^a and Geoffrey Bodenhausen^{adef}

Complex overlapping multiplets due to scalar couplings ${}^nJ(^{13}\text{C}, ^{13}\text{C})$ in fully ^{13}C -enriched molecules can be simplified by polychromatic irradiation of selected spins. The signal intensities of the remaining non-irradiated signals are proportional to the concentrations, as shown in this work for the anomeric ^{13}C signals of the α - and β -conformers of glucose. Homonuclear decoupling can therefore be useful for quantitative NMR studies. The resulting decoupled lineshapes show residual fine structures that have been investigated by means of numerical simulations. Simulations also show that homonuclear decoupling schemes remain effective despite inhomogeneous static fields that tend to hamper *in cellulo* and *in vivo* studies. Homonuclear decoupling schemes can be combined with dissolution DNP to obtain signal enhancements of more than four orders of magnitude. Polychromatic irradiation of selected spins does not cause significant losses of hyperpolarization of the remaining non-irradiated spins.

Received 21st December 2015,
Accepted 21st March 2016

DOI: 10.1039/c5cp07884a

www.rsc.org/pccp

Introduction

For molecules such as polysaccharides, proton spectra tend to be crowded. By comparison, ^{13}C spectra of fully enriched compounds offer a better spectral dispersion. However, homonuclear scalar ${}^nJ(^{13}\text{C}, ^{13}\text{C})$ couplings may lead to extensively overlapping multiplets. We propose to use homonuclear polychromatic decoupling during the acquisition of ^{13}C signals to reduce the complexity of spectra of fully ^{13}C -enriched compounds. This proves to be helpful to extract information regarding concentrations, *e.g.*, for equilibria between α - and β -anomers of saccharides, and kinetic studies of reactions like enzymatic phosphorylations.

A simple (though in many cases more expensive) expedient to eliminate multiplets altogether is by choosing selective labeling, *e.g.*, by studying saccharides that are only ^{13}C -enriched in the anomeric $^{13}\text{C}^1$ position. Indeed, this allows one to study the

kinetics of the enzymatic phosphorylation of glucose.¹ But when subsequent steps in the pentose phosphate pathway (PPP) must be investigated, the $^{13}\text{C}^1$ carbon is eliminated as $^{13}\text{CO}_2$, so that the remaining molecule only contains ^{12}C isotopes. Such processes make it desirable to start with fully ^{13}C -enriched compounds.

Homonuclear decoupling techniques have been known for decades.^{2–4} So far, these techniques have been mostly used to simplify multiplets in proton spectra. We recently described a novel method dubbed Window-Acquired Spin-Tailoring Experiment (WASTE) that allows one to decouple several homonuclear scalar interactions simultaneously.⁵ When very weak radio-frequency (rf) fields are employed, the progressive or regressive connectivities of selected transitions can be identified by ‘spin tickling’ effects.⁶ Both homonuclear decoupling and tickling methods use combs of short pulses (typically 1 μs) that are inserted in the dwell times between the intervals where the receiver is activated to acquire the free induction signal. The effective irradiation frequency of each comb of pulses can be controlled by shifting the rf phase between the pulses that make up the comb, so as to irradiate near the chemical shift of a selected spin. A superposition of m combs of pulses allows one to irradiate m selected spins simultaneously. The average rf field strength of each of the m combs must be approximately equal to the magnitude of the scalar coupling constants that one wishes to decouple. In contrast to earlier work on decoupling of weak homonuclear couplings $0 < {}^nJ(^1\text{H}, ^1\text{H}) < 15$ Hz, in this study we investigate the performance of our decoupling scheme

^a Institut des sciences et ingénierie chimiques (ISIC),
Ecole Polytechnique Fédérale de Lausanne (EPFL), CH-1015 Lausanne, Switzerland

^b Department of Chemistry, School of Chemical Sciences,
Central University of Karnataka, Gulbarga, 585311 Karnataka, India

^c Neuchâtel Platform of Analytical Chemistry (NPAC), Institut de Chimie,
Université de Neuchâtel, Avenue de Bellevaux 51, 2000 Neuchâtel, Switzerland.
E-mail: diego.carnevale@unine.ch

^d École Normale Supérieure-PSL Research University, Département de Chimie,
24 rue Lhomond, F-75005 Paris, France

^e Sorbonne Universités, UPMC Univ Paris 06, LBM, 4 place Jussieu, F-75005, Paris,
France

^f CNRS, UMR 7203 LBM, F-75005, Paris, France

† Electronic supplementary information (ESI) available. See DOI: 10.1039/c5cp07884a

on larger couplings $^1J(^{13}\text{C}, ^{13}\text{C}) \approx 40$ Hz, which require substantially higher average rf fields, and which are often superimposed with much smaller long-range couplings $^2J(^{13}\text{C}, ^{13}\text{C}) < 5$ Hz. Yet the average rf field of each comb remains small enough so that one can incorporate at least $m = 10$ pulses in each dwell time to decouple at m frequencies simultaneously. We refer to such experiments as polychromatic irradiations. In this work, we combine homonuclear decoupling with dissolution dynamic nuclear polarization (D-DNP). This technique can be utilized to boost the signal intensity in kinetic studies aimed at monitoring enzymatic reactions or metabolic pathways as a function of time, both *in vitro* and *in vivo*. In such studies, decoupling methods should preserve the hyperpolarized magnetization while the chemical kinetics that one wishes to monitor take place. It is common practice to use only pulses with small nutation angles $\beta < 5^\circ$ to monitor T_1 decays or build-up times of enzymatic reactions and metabolic pathways with hyperpolarized magnetization. Pulses with larger nutation angles should be avoided since they lead to losses of polarization.

In various established techniques for homonuclear decoupling, the signals are observed in a window-acquired fashion,^{7–11} in a pseudo-2D manner,^{12,13} or by combining in-phase and anti-phase multiplets in complementary spectra.^{14,15} Most of these techniques utilize soft π pulses to invert selected nuclear spins while leaving their coupling partners unperturbed to refocus J -couplings. However, the use of π pulses is not compatible with hyperpolarized samples, in particular for kinetic studies, since the polarization would be attenuated. Decoupling techniques that require combinations of complementary experiments are not suitable for kinetic studies.

Our polychromatic decoupling technique is particularly promising with respect to the above requirements. In fact, it can be applied ‘on-the-fly’ in a single experiment by virtue of its window-acquired nature and causes minimal perturbations of the hyperpolarized magnetization by virtue of the minimal rf pulses delivered to the sample. Decoupling of either homonuclear or heteronuclear scalar interactions is achieved by means of very short pulses (typically 1 μs) with low rf power and small flip angles (typically 1°). In fact, as we have proven by means of average Hamiltonian theory, complete decoupling can be achieved when the condition $\langle \nu_1 \rangle = J/2$ is met, *i.e.*, when the rf-field strength has half the magnitude of the scalar interaction that one needs to decouple.⁵ This latter condition holds for both weakly- and strongly-coupled spin systems. Very short pulses do not bring about any significant nutation but act in the manner of weak spin-locking pulses. A combination of homonuclear proton decoupling based on the BIRD method¹⁶ and signal enhancement by DNP has recently been reported for systems where the proton magnetization is generated by cross relaxation from hyperpolarized ^{13}C nuclei.¹⁷ This technique cannot be utilized for homonuclear decoupling of ^{13}C -enriched samples. BIRD decoupling cannot be used to follow kinetics, since DNP-enhanced ^{13}C polarization is destroyed in the first decoupling experiment.

We show that polychromatic irradiation of selected spins does not cause significant losses of hyperpolarization of the

remaining non-irradiated spins. This opens the way to simplifying multiplets in spectra that are enhanced by at least four orders of magnitude.

Results and discussion

A sample of fully ^{13}C -enriched deuterated glucose was chosen to demonstrate the advantages of homonuclear decoupling in ^{13}C NMR. Deuterated glucose has longer relaxation times $T_1(^{13}\text{C})$ than ordinary glucose, which makes it more suitable for dissolution dynamic nuclear polarization (D-DNP). The long lifetimes of longitudinal magnetization $S_z(^{13}\text{C})$ of hyperpolarized deuterated glucose allowed us to determine the rates of the enzymatic phosphorylation of both α - and β -anomers of glucose by hexokinase.¹ In contrast to views that appear to be widely accepted in enzymology, we found that the phosphorylation rates of the α - and β -anomers of glucose are very similar. Such studies rely on the integration of the amplitudes of ^{13}C signals that are generally proportional to the concentrations (‘quantitative’ in analytical jargon). However, partly overlapping multiplets may render signal integration difficult. We therefore decided to apply homonuclear polychromatic decoupling methods to simplify the carbon multiplets that are due to scalar couplings $^nJ(^{13}\text{C}, ^{13}\text{C})$, with $n = 1$ and 2, in ^{13}C -enriched deuterated glucose.

The ^{13}C spectrum of glucose reflects the superposition of the two α - and β -anomers that are in slow chemical exchange and have relative concentrations $[\alpha]:[\beta] = 36:64$ in aqueous solution at room temperature. The ^{13}C spectrum contains no fewer than twelve multiplets due to short-range couplings $^1J(C^i, C^j) \sim 50$ Hz that are broadened by long-range couplings $^2J(C^i, C^j) \approx 5$ Hz and $^3J(C^i, C^j) \approx 5$ Hz. The pulse sequence used for polychromatic homonuclear decoupling of ^{13}C nuclei combined with ^2H decoupling is shown in Fig. 1. For a typical spectral width 12.5 kHz, one can easily accommodate about $m = 10$ pulses with a duration $\tau_p = 1 \mu\text{s}$ in each dwell time $\Delta t = 80 \mu\text{s}$.

In order to simplify a multiplet of interest, one needs to irradiate only the relevant coupling partners. Therefore the chemical shifts of all spins that are responsible for the multiplets need to be known. By way of demonstration, Fig. 2 shows how two small doublets-of-doublets that constitute submultiplets of the C-1 α multiplet can be irradiated simultaneously, resulting in a simplification of both multiplets C-5 α and C-6 α . This confirms that the doublets-of-doublets of C-1 α are due to couplings with C-5 α and C-6 α . In this way, we can verify the coupling partners of each multiplet and, consequently, determine the coupling constants in the remaining multiplets that are left once a chosen interaction has been decoupled. The J -couplings that we determined are listed in Table 1. They are in good agreement with earlier work.¹⁸

For kinetic studies, *e.g.*, to monitor the rates of phosphorylation of the α - and β -anomers of glucose by hexokinase,^{19,20} it is sufficient to integrate a single peak in each isomer. The anomeric C-1 α and C-1 β signals are attractive in this respect since they do not overlap with the rest of the spectrum. In order to collapse the multiplets of the two anomeric C-1 α and C-1 β sites to singlets,

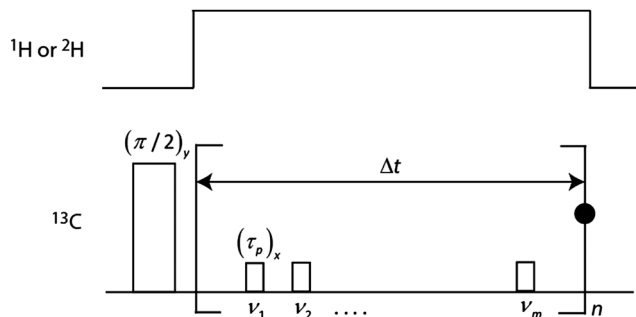


Fig. 1 Pulse scheme for polychromatic homonuclear ^{13}C - ^{13}C decoupling with m distinct irradiation frequencies. The sequence can be combined with heteronuclear ^1H and/or ^2H decoupling. The duration τ_p of each decoupling pulse is typically 1 μs . In each of the n dwell times Δt , m decoupling pulses with effective frequencies $\nu_1, \nu_2, \dots, \nu_m$ are applied, until the total acquisition time $n\Delta t$ is completed. The frequency of each comb of pulses, *i.e.*, the offset $\Delta\nu_m = \nu_m - \nu_0$ with respect to the rf carrier ν_0 is determined by shifting the phase of the k th pulse belonging to the m th comb through $\phi_{k,m} = k\Delta\phi_m$ where the phase shift is $\Delta\phi_m = 2\pi\Delta\nu_m/\Delta t$. The black dot represents a single acquisition point or a suitable interval where the receiver may be activated to allow for averaging. A total of n data points are acquired in n dwell times, each of which must have a duration $\Delta t = 80 \mu\text{s}$ if the desired spectral width is 12.5 kHz. The positions of the m decoupling pulses within a given dwell time and the delays between these pulses are immaterial, provided the electronics are capable of executing the pulse program accurately. The interval between two consecutive pulses belonging to the same comb irradiating at frequency ν_m is always equal to the dwell time Δt . A pulse program for a Bruker AVANCE-1 system is given in ESI.†

we have to simultaneously irradiate all coupling partners, *i.e.*, the three partners C-2 α , C-5 α , C-6 α of the α -anomer, and at the same time the three partners C-2 β , C-3 β and C-6 β of the β -anomer. As Fig. 3 demonstrates, the multiplets of the anomeric C-1 α and C-1 β signals can be simplified stepwise. The removal of large short-range couplings $^1J \sim 50$ Hz requires stronger average rf fields $\langle\nu_1\rangle \approx 80$ Hz than are needed for the long-range couplings $^2J \sim 5$ and $^3J \sim 5$ Hz. To remove larger couplings, irradiation at the isotropic shift $\nu_{\text{rf}} = \delta_{\text{iso}}$ is sufficient, whereas the irradiation of submultiplets (*i.e.*, at frequencies $\nu_{\text{rf}} = \delta_{\text{iso}} \pm ^1J/2$) is sufficient to remove small long-range couplings. The two cases of strong and weak rf fields are indicated in Fig. 3 by filled and open triangles, respectively. It is worth stressing at this point that, when the larger 1J is removed, the smaller long-range 2J and 3J couplings are also decoupled, whereas one can remove small long-range 2J and 3J couplings with weak rf fields without affecting the multiplets due to 1J . In cases where multiplets due to different carbons are heavily overlapped, a single strong rf field may remove all interactions of the overlapping resonances. For instance, in our sample, the submultiplets of C-6 β and C-6 α happen to be heavily overlapped, as well as the three submultiplets of C-2 α and C-5 α , C-4 α and C-4 β , and C-5 β and C-3 β . Fig. 3a and e show the unperturbed C-1 β and C-1 α multiplets, respectively. Fig. 3b and f demonstrate the collapse of the multiplets of C-1 β and C-1 α due to irradiation of C-6 β and C-5 α , respectively. Fig. 3c and g show how the multiplets can be further simplified when all three sites C-3 β , C-6 α and C-6 β are irradiated simultaneously. The complete

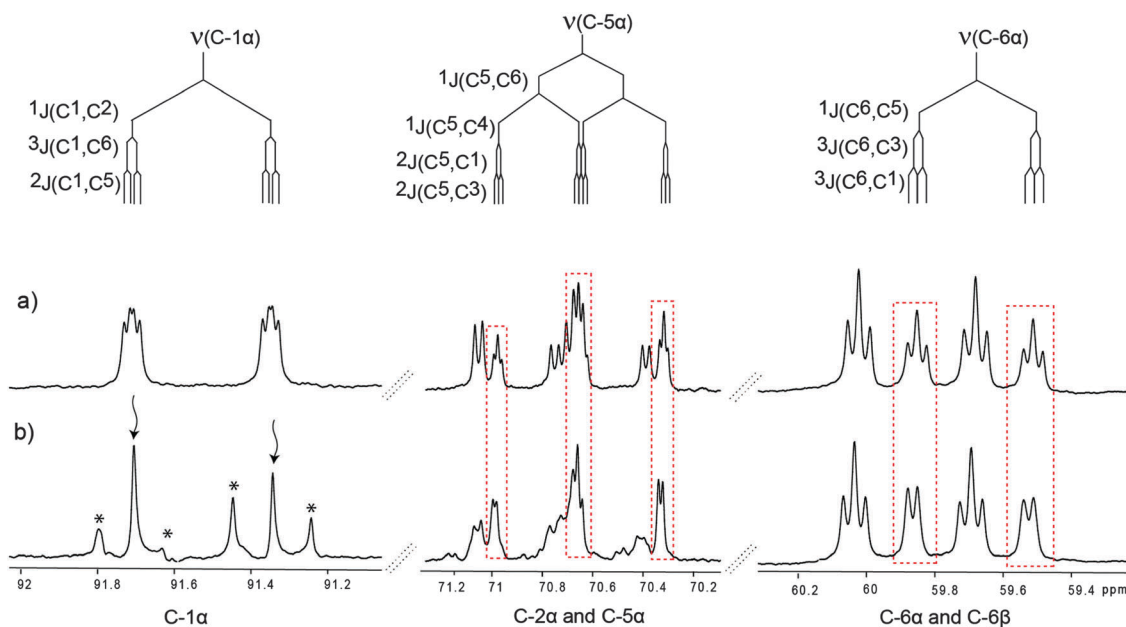


Fig. 2 (a) Multiplets extracted from the conventional ^{13}C spectrum of fully ^{13}C -enriched deuterated glucose with ^2H decoupling. (b) Decoupling of small long-range interactions between C-1 α and its coupling partners C-5 α and C-6 α , achieved by two weak rf fields ($m = 2$) each with an average rf field strength $\langle\nu_1\rangle = 10$ Hz, *ca.* twice the sum $^2J(\text{C}^1, \text{C}^5) + ^3J(\text{C}^1, \text{C}^6) = 1.8 + 3.2$ Hz = 5 Hz, centered on the two submultiplets of C-1 α (wavy arrows) that arise from the large splitting $^1J(\text{C}^1, \text{C}^2) = 45.5$ Hz. Because of the resulting decoupling of both $^2J(\text{C}^1, \text{C}^5)$ and $^3J(\text{C}^1, \text{C}^6)$, the multiplets C-5 α (framed in dashed red rectangles) are partly simplified, leaving multiplet structures due to $^1J(\text{C}^5, \text{C}^6) = 42.5$, $^1J(\text{C}^5, \text{C}^4) = 38.6$ and $^2J(\text{C}^5, \text{C}^3) = 1.8$ Hz, while C-6 α (also framed in dashed red rectangles) shows a multiplet structure caused by $^1J(\text{C}^6, \text{C}^5) = 42.5$ and $^3J(\text{C}^6, \text{C}^3) = 3.4$ Hz. Asterisks in (b) indicate artifacts due to the rf irradiation.

Table 1 Scalar couplings ${}^nJ(C^i, C^j)$ in α - and β - $^{13}\text{C}_6\text{d}_7$ -glucose in a 0.3 M aqueous solution at 298 K (25 °C). All scalar coupling constants are given in Hz. The ${}^2J(C^i, C^j)$ and ${}^3J(C^i, C^j)$ couplings are represented by double-headed red arrows in the graphs. Symbols ε indicate couplings that are too small to be observed

	C ²	C ³	C ⁴	C ⁵	C ⁶
α-Glucose					
C ¹	45.5	ε	ε	1.8	3.2
C ²		38.4	3.4	ε	ε
C ³			38.5	1.8	3.4
C ⁴				38.6	ε
C ⁵					42.5

β-Glucose					
C ¹	45.5	4.8	ε	ε	4.1
C ²		38.6	3.1	ε	ε
C ³			39.2	2.3	4.1
C ⁴				39.2	ε
C ⁵					42.5

collapse of the two C-1 β and C-1 α multiplets to mere singlets is shown in 3d and h, which occurs when all coupling partners are irradiated at the same time. The vertical dashed lines indicate the isotropic shifts of the anomeric C-1 β and C-1 α carbons. As expected, Bloch–Siegert shifts are observed when the number and amplitude of the rf fields increases.^{21–23} The largest shifts are observed when moving from (c) to (d) and from (g) to (h). In the latter two cases, two additional stronger rf pulse trains were used to remove the larger 1J couplings with C-2 β and C-2 α . These stronger pulses also remove the smaller 2J interaction with the overlapped C-5 α . It is important to note that the ratio of the integrals is preserved despite polychromatic decoupling, showing that the technique can be used for quantitative analysis.

The decoupled multiplets of C-1 α in Fig. 3b–d show fine structures that are not fully resolved due to homogeneous and inhomogeneous broadening. These fine structures are not expected in ‘linear’ coupling networks that are made up of simple chains of coupled nuclei. In fully ^{13}C -enriched molecules, the coupling networks are only ‘linear’ in the (unrealistic) case that all long-range couplings ${}^nJ(C^i, C^j)$ with $n > 1$ can be neglected, *i.e.*, when only one-bond couplings with $n = 1$ between neighboring nuclei occur. In this respect, ^{13}C -enriched molecules are more challenging than systems with coupled protons, which are often ‘linear’ since it is usually sufficient to consider only vicinal ${}^nJ(\text{H}^i, \text{H}^j)$ couplings with $n = 3$. Indeed, in our previous studies of homonuclear decoupling in proton NMR, simple

singlets could be obtained (albeit accompanied by weak ‘tickling sidebands’) when the condition $\langle \nu_1 \rangle = J/2$ was approximately satisfied. In a ^{13}C -enriched sample, however, we must also consider long-range couplings ${}^nJ(C^i, C^j)$ with $n > 1$. Referring to the α - and β -anomers of glucose described in Table 1, the spin systems are clearly not ‘linear’ and their coupling topologies have ‘cyclic’ properties with respect to scalar interactions.

In order to investigate the effects of polychromatic decoupling on such systems, numerical simulations were carried out with the SIMPSON program.²⁴ A three-spin system was considered with chemical shifts $\nu_A = 0$, $\nu_M = 1$, and $\nu_X = 3$ kHz, and scalar coupling constants ${}^1J(A, M) = 50$, ${}^1J(M, X) = 40$ and ${}^2J(A, X) = 10$ Hz (Fig. 4). The multiplets of spins X and M in the unperturbed spectrum without decoupling are shown in Fig. 4a. The spectrum resulting from the application of an rf field with $\nu_{\text{rf}} = \nu_A$, $\tau_p = 1$ μs , $\Delta t = 100$ μs and an average rf field strength $\langle \nu_1 \rangle = \nu_1 \tau_p / \Delta t = 100$ Hz is shown in Fig. 4b. Broadly speaking, we indeed observe the expected collapse of the ${}^1J(A, M)$ and ${}^2J(A, X)$ splittings, while the splitting due to ${}^1J_{MX}$ is still present. However, an unexpected fine structure appears. Surprisingly, the high-frequency (left) part of spin X appears as a doublet with a splitting of 2.73 Hz and the low-frequency part as a doublet with a splitting of 1.88 Hz. The high-frequency part of spin M is split into a doublet with a splitting of 6.92 Hz and the low-frequency part split into a doublet with a splitting of 2 Hz. To collapse the multiplet of spin M to a simple singlet, it is necessary to irradiate both A and X. Likewise, spin X can be reduced to a singlet by irradiating both A and M as shown in Fig. 4d. The Bloch–Siegert effects observed in the experimental spectra of Fig. 3 can also be seen *in silico*. These are known to be proportional to the square of the strength of the rf field, and inversely proportional to the shift between the observed and irradiated spins.^{21–23} To illustrate these coherent effects, some numerical simulations of dichromatic decoupling experiments are given in Fig. S1 of the ESI.† These simulations highlight the appearance of additional splittings, rf-related artifacts and asymmetric line-shapes upon irradiation of coupling partners, similar to those observed in Fig. 2 and 3.

The effect of the inhomogeneity of the static field on the performance of our polychromatic decoupling scheme has also been investigated. A series of spectra has been simulated where the chemical shifts of all spins (or, equivalently, both carrier and receiver frequencies) are incremented in concert over an interval $\Delta\nu = \pm 10$ Hz around the average shifts $\nu_A = 0$, $\nu_M = 1$ and $\nu_X = 3$ kHz. This series of spectra represents a rectangular distribution of spins centered about the on-resonance condition. A Lorentzian function with a width at half height of 2 Hz, also centered on the average shifts, was used to weight the rectangular distribution. Subsequently, all weighted spectra are added to mimic a spectrum that one would obtain in an inhomogeneous B_0 field characterized by a Lorentzian distribution with a width at half height of 2 Hz. The effect on the spectra is shown in Fig. 4c and e, respectively. These simulations show that such a broadening can easily mask small splittings due to tickling effects, as observed in the experimental spectra of Fig. 3.

The possibility of using polychromatic ^{13}C – ^{13}C decoupling *in cellulo* is particularly appealing. In such systems, the

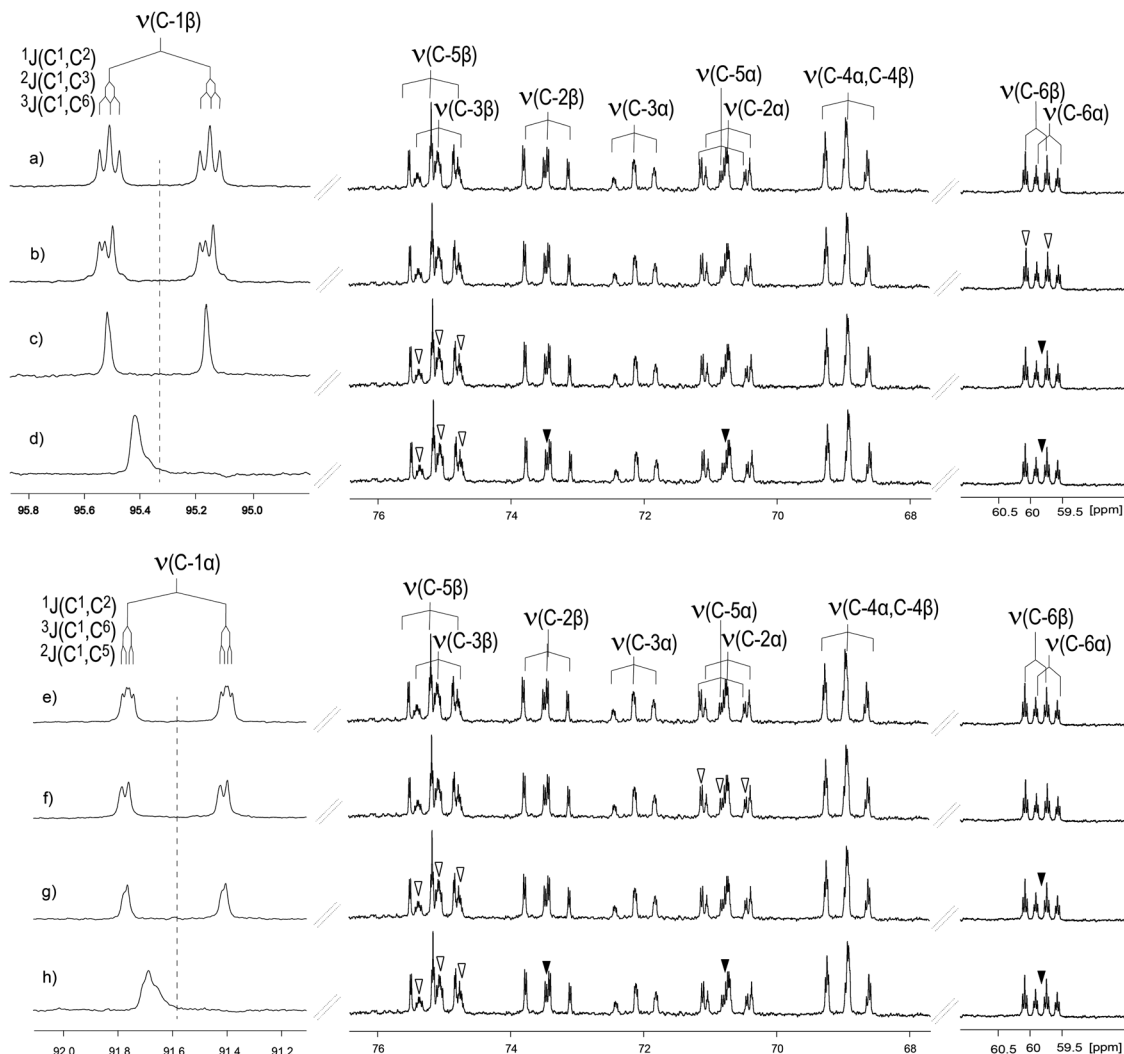


Fig. 3 Spectra of fully ^{13}C -enriched deuterated glucose with ^2H decoupling. (left) Partly decoupled multiplets and (middle and right) irradiation frequencies indicated by triangles superimposed onto undecoupled spectra. Filled triangles represent strong average rf fields ($100 < \langle \nu_1 \rangle < 200$ Hz) for decoupling 1J whereas open triangles represent weak average rf fields ($5 < \langle \nu_1 \rangle < 20$ Hz) for decoupling 2J or 3J . Stepwise simplifications of the multiplets C-1 β (b)–(d) and C-1 α (f)–(h) are achieved by polychromatic decoupling with different frequencies ν_m . The collapse of the C-1 β and C-1 α multiplets to doublets (c) and (g) or to singlets (d) and (h) can be achieved in a single polychromatic experiment with $m = 4$ or 6 frequencies, respectively, addressing the relevant peaks of both anomers, as shown in (c) and (g), or (d) and (h), respectively. (a and e) Conventional ^{13}C spectrum without homonuclear decoupling. (b) Polychromatic decoupling of C-6 β ($m = 2$, $\langle \nu_1 \rangle = 4.2$ Hz) removes the $^3J(\text{C}^1, \text{C}^6)$ interaction. (f) Decoupling of C-5 α ($m = 3$, $\langle \nu_1 \rangle = 3.5$ Hz) removes $^2J(\text{C}^1, \text{C}^5)$. (c and g) Decoupling of C-3 β ($m = 3$, $\langle \nu_1 \rangle = 16$ Hz) removes the $^2J(\text{C}^1, \text{C}^3)$ interaction while decoupling of C-6 β and C-6 α ($m = 1$, $\langle \nu_1 \rangle = 92$ Hz) removes the $^3J(\text{C}^1, \text{C}^6)$ interaction. (d and h) Decoupling of C-2 β ($m = 1$, $\langle \nu_1 \rangle = 100$ Hz) removes the $^1J(\text{C}^1, \text{C}^2)$ interaction, decoupling of C-3 β ($m = 3$, $\langle \nu_1 \rangle = 10$ Hz) removes the $^2J(\text{C}^1, \text{C}^3)$ interaction, decoupling of C-6 β and C-6 α ($m = 1$, $\langle \nu_1 \rangle = 92$ Hz) removes $^3J(\text{C}^1, \text{C}^6)$ and decoupling of C-2 α and C-5 α ($m = 1$, $\langle \nu_1 \rangle = 180$ Hz) removes $^1J(\text{C}^1, \text{C}^2)$ and $^2J(\text{C}^1, \text{C}^5)$ interactions. The total average rf field employed in the spectrum of (d) and (h) was $\langle \nu_1 \rangle_{\text{tot}} = (100 + 3 \times 10 + 92 + 180)$ Hz = 402 Hz. The vertical dotted lines on the left indicate the chemical shift of the multiplets C-1 β and C-1 α before decoupling. The shifts are due to Bloch–Siegert effects that depend on the offsets and the average rf amplitude ($\langle \nu_1 \rangle$). In (c) and (g) the same spectrum is shown twice, obtained with a single experiment with $m = 4$ so that the multiplets of C-1 of both α and β anomers collapse to doublets. In (d) and (h) the same spectrum is shown twice, obtained with a single experiment with $m = 6$ that causes the multiplets of C-1 of both anomers to collapse to singlets.

inhomogeneity of the external magnetic field is much larger than in isotropic solutions. In order to evaluate the performance of our decoupling scheme in inhomogeneous magnetic fields, simulations analogous to those of Fig. 4 have been carried out assuming a ten-fold larger B_0 inhomogeneity, represented by a Lorentzian distribution of shifts with a width at half height of 20 Hz. The resulting spectra are shown in Fig. 5. Although the lineshapes obtained are substantially broader than those of

Fig. 4, one can easily appreciate that the efficiency of decoupling does not break down. Thus homonuclear decoupling schemes remain effective despite inhomogeneous static fields that tend to hamper *in cellulo* and *in vivo* studies. These results are promising in view of future applications to cell suspensions.

Our polychromatic decoupling method can be combined with dissolution dynamic nuclear polarization (D-DNP).^{25,26} In this context, it is important to preserve the enhanced polarization.

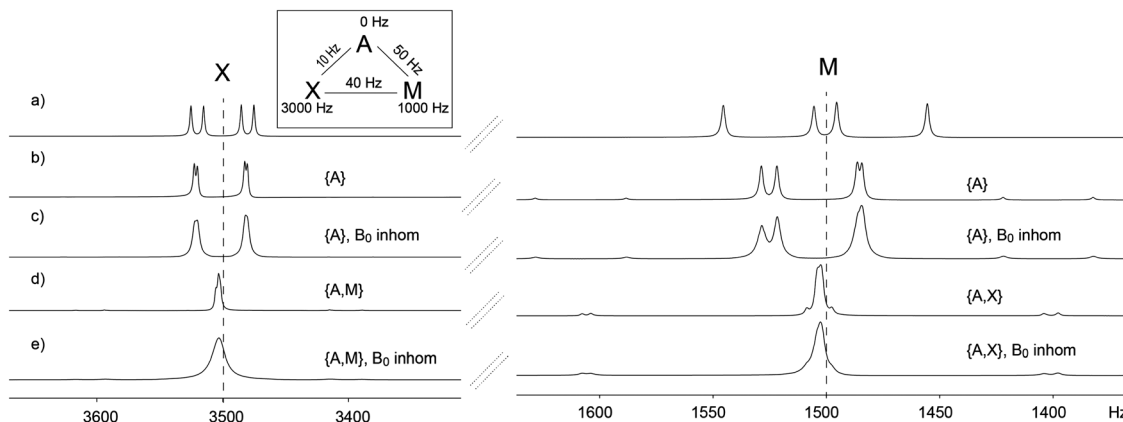


Fig. 4 (a) Simulations of the multiplets of spins X and M of a typical AMX system without decoupling. (b) X and M spin multiplets with monochromatic decoupling of spin A in a homogeneous magnetic field and (c) in an inhomogeneous magnetic field described by a Lorentzian distribution of chemical shifts, with a width at half height of 2 Hz. (d) X and M spin multiplets with polychromatic decoupling of both spins A and M (left), and of both spins A and X (right) in a homogeneous magnetic field. (e) Idem in an inhomogeneous magnetic field. The average rf field strength $\langle \nu_1 \rangle = 100$ Hz is equal to twice the largest scalar coupling $^1J(A, M) = 50$ Hz. Vertical dashed lines indicate the chemical shifts of X and M spins without decoupling, when they are not affected by Bloch–Siegert effects.

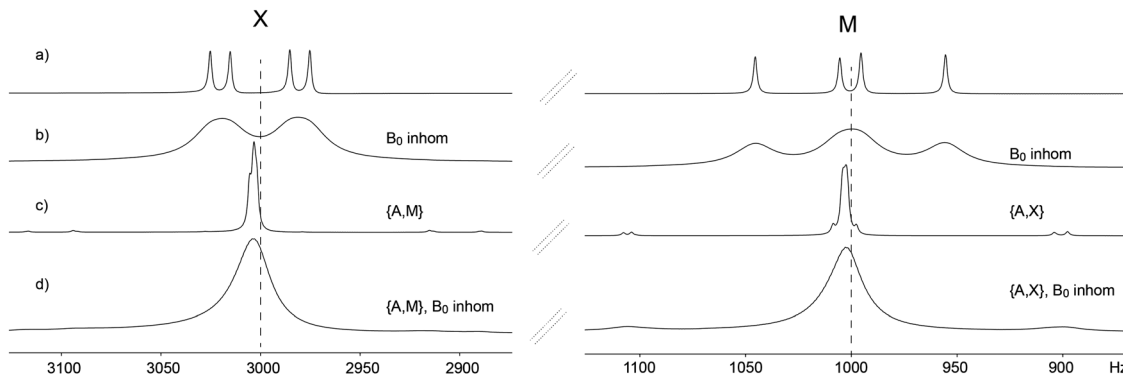


Fig. 5 (a–d) Simulations of multiplets of spins X and M of an AMX system similar to Fig. 4 but in a more severely inhomogeneous magnetic field described by a Lorentzian distribution of chemical shifts with a width at half height of 20 Hz.

In order to be eligible for hyphenation by DNP, our decoupling scheme should not perturb the populations of non-irradiated spins. We performed $T_1(^{13}\text{C})$ inversion-recovery experiments with and without a comb of rf pulses of duration $\tau_p = 1$ μs spaced by $\Delta t = 50$ μs (duty cycle $\tau_p/\Delta t = 2\%$), inserted in the inversion-recovery delay τ_{IR} that separates the 180° and 90° pulses, which has been incremented up to $\tau_{\text{IR}} = 50$ s. The effective rf frequencies of the two combs were at offsets -1136 Hz with respect to the chemical shift of C-1 α , and -1607 Hz with respect to C-1 β . An rf field strength $\nu_1 = 1$ kHz was used, corresponding to an average rf field $\langle \nu_1 \rangle = \nu_1 \times \tau_p/\Delta t = 20$ Hz. These conditions are similar to the experiments of Fig. 2–4 for the removal of long-range couplings. The $T_1(^{13}\text{C})$ values are substantially identical with and without comb of rf pulses in the inversion-recovery delays τ_{IR} . More specifically, $T_1(\text{C-1}\alpha) = 9.07 \pm 0.05$ s without and 9.06 ± 0.05 s with rf irradiation. For the other anomer, $T_1(\text{C-1}\beta) = 9.43 \pm 0.04$ without and 9.50 ± 0.07 s with rf irradiation. Thus, in the case of moderate average field strengths, the intensities of the signals are not perturbed by the irradiation scheme. These results show that

our decoupling scheme can be applied to hyperpolarized states without compromising the DNP enhancement.

The performance of homonuclear decoupling schemes in combination with dissolution dynamic nuclear polarization (D-DNP) techniques was investigated experimentally. A sample comprising of ^{13}C -enriched fully-deuterated glucose with 40 mM of TEMPOL in $\text{D}_2\text{O}:\text{H}_2\text{O}:\text{glycerol-d}_6$ was used to prepare frozen pellets which were subsequently polarized at 1.2 K in a 6.7 T magnet by means of microwave irradiation at 188.3 GHz. Once polarized by means of $^1\text{H} \rightarrow ^{13}\text{C}$ cross-polarization,²⁷ the sample was dissolved with 5 mL of superheated H_2O and pushed in 6 s towards a high-resolution spectrometer operating at 11.75 T (500 MHz for ^1H). After a waiting time of 4 s needed for the sample to fill the NMR tube, 5° pulses were applied to ^{13}C at 1 s intervals followed by acquisition with (i) and without (ii) our homonuclear ^{13}C decoupling scheme. In both cases, deuterium was decoupled during acquisition. The normalized spectra of the C-1 α and C-1 β in glucose under conditions (i) and (ii) are shown in Fig. 6a in blue and red, respectively. The residual splitting observed on the C-1 β resonance indicates non-ideal decoupling

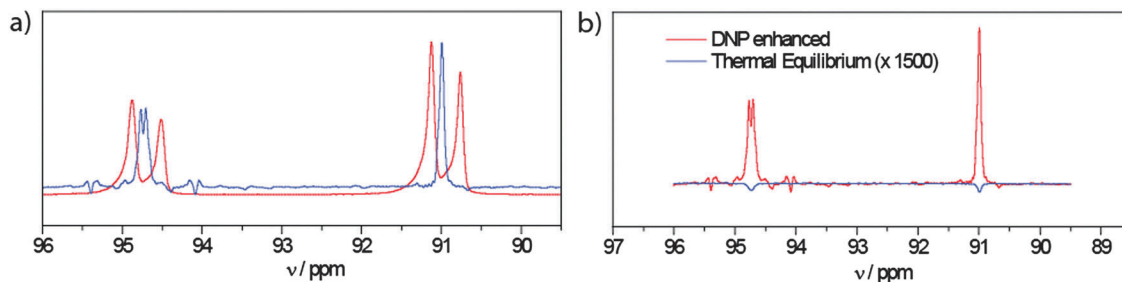


Fig. 6 (a) C_1 region of a DNP-enhanced ^{13}C spectrum of ^{13}C -enriched glucose- d_7 acquired after dissolution. Spectra with and without homonuclear decoupling are shown in blue and red, respectively. (b) Decoupled spectra analogous to those of Fig. 3(d) and (h), used to estimate the ratio of D-DNP enhanced with respect to non-enhanced spectra in thermal equilibrium, shown in red and blue, respectively.

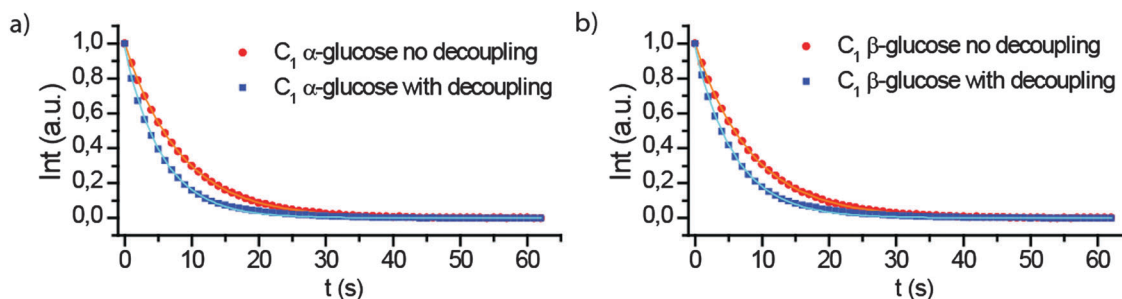


Fig. 7 (a) Measurement of $T_1(C-1\alpha)$ of ^{13}C -enriched d_7 -glucose enhanced by D-DNP with and without homonuclear decoupling, in blue and red, respectively. (b) Similar measurement for $T_1(C-1\beta)$. Decoupling conditions were analogous to those required for complete decoupling of both $C-1\alpha$ and $C-1\beta$ multiplets in a hexachromatic ($m = 6$) irradiation experiment as in Fig. 3(d) and (h), employing a total average rf intensity $\langle\nu_1\rangle = 420$ Hz.

due to small variations of the transmitter frequency relatively to the relevant shifts. This is ascribed to the fact that field-frequency lock using the 2H channel was not utilized in the experiments of Fig. 6a and b. In order to estimate the enhancement achieved by DNP, a decoupled spectrum was acquired at thermal equilibrium with a 90° pulse followed by a comb of rf pulses. The resulting spectrum is shown in blue in Fig. 6b, where the DNP-enhanced spectrum is displayed in red for comparison. The DNP enhancements were estimated to be *ca.* 42 000 for α -glucose and *ca.* 32 000 for β -glucose. The blue spectrum appears in negative adsorption mode to indicate that the DNP enhancements obtained in these experiments were negative.

The relaxation time constants of the hyperpolarized signal were determined under conditions (i) and (ii). For deuterated α -glucose, $T_1(C-1\alpha) = 8.25 \pm 0.02$ s without irradiation and $T_1(C-1\alpha) = 5.6 \pm 0.1$ s with trains of rf pulses (Fig. 7a). Similarly, for β -glucose, $T_1(\beta-C^1) = 8.44 \pm 0.02$ s and $T_1(C-1\beta) = 5.9 \pm 0.1$ s (Fig. 7b). In these decoupling experiments the average rf field was that required for complete decoupling of the $C-1\alpha$ and $C-1\beta$ multiplets as in Fig. 3(d) and (h), *i.e.*, $\langle\nu_1\rangle = 420$ Hz. As a result, in contrast with the T_1 measurements performed with inversion-recovery experiments employing weak irradiation with $\langle\nu_1\rangle = 20$ Hz, the longitudinal relaxation time constants were decreased by *ca.* 32% and 30% for α - and β -glucose, respectively. The resulting decrease in the life-times of the polarization is not dramatic and suggests that polychromatic decoupling schemes may be freely utilized in combination with dissolution DNP experiments, although small average rf fields

must be recommended. In practice, the effect of polychromatic decoupling on the hyperpolarization can be reduced by choosing an acquisition time (*i.e.*, the time when decoupling takes place) that does not exceed $1/\Delta\nu$, where $\Delta\nu$ is the inhomogeneous linewidth of the resonance that one wishes to observe.

Conclusions

In summary, we can simplify multiplets due to ^{13}C - ^{13}C couplings in fully ^{13}C -enriched deuterated α - and β -glucose without loss of quantitative information, so that the ratio of the integrals of the non-irradiated signals faithfully reflects the relative concentrations of the α and β anomers. The broadening of the decoupled lines is due to tickling effects that occur in systems with 'non-linear' coupling networks. Numerical simulations prove that our method is robust with respect to inhomogeneous B_0 fields, so that *in cellulo* NMR studies should be possible. T_1 measurements performed in the presence of weak off-resonance irradiation show that weak rf fields do not significantly affect the longitudinal relaxation rate, so that the hyperpolarization that can be achieved by DNP is preserved. However, when larger average rf fields are required to fully decouple several resonances of interest, polychromatic rf irradiation techniques may accelerate the decay of hyperpolarization. Thus, polychromatic decoupling can be combined with DNP enhancement, provided some care is taken to limit the rf field strengths.

Experimental details

All spectra were acquired on a Bruker Avance-I spectrometer equipped with a 11.7 T magnet (125 MHz for ^{13}C) and a triple-channel 'cryoprobe' suitable for deuterium decoupling. All conventional NMR experiments were performed at room temperature, with typical recovery delays of 10 s and 90° pulse lengths of 11.8 μs corresponding to an rf field strength of 21 kHz for ^{13}C . The spectral width of 12.5 kHz corresponds to a dwell time $\Delta t = 80 \mu\text{s}$. The effective frequency of the m th comb can be shifted with respect to the carrier frequency ν_{rf} by a shift $\Delta\nu_m = \Delta\phi_m/(2\pi\Delta t)$ where $\Delta\phi_m$ is a phase increment, so that the k th pulse of the m th comb has a phase $\phi_{km} = k\Delta\phi_m$, where $k = 1, 2, \dots, n$ is the index of the data points acquired in the course of n dwell times Δt .^{5,28–32} The length of the pulses was $\tau_p = 1 \mu\text{s}$ in all cases, with rf field strengths for each individual comb in the range $0.3 < \nu_1 < 14.4$ kHz, corresponding to cumulative average rf field strengths utilized in polychromatic irradiations ($1 \leq m \leq 6$) in the range $20 < \langle \nu_1 \rangle < 420$ Hz. A WALTZ-16³³ sequence was used to decouple the ^2H nuclei. The ^{13}C -enriched deuterated glucose was purchased from Cortecnet. The numerical simulations shown in Fig. 4 and 5 were carried out with SIMPSON.²⁴

For the DNP experiments, a volume of 100 μL of 1.5 M [$^{13}\text{C}_6, \text{d}_7$]-glucose in $\text{D}_2\text{O}:\text{H}_2\text{O}:\text{glycerol-d}_6$ 3:2:5 containing 40 mM TEMPOL was polarized at $B_0 = 6.7$ T and $T = 1.2$ K by microwave irradiation at 188.3 GHz (negative polarization) using 10 kHz frequency modulation swept over a bandwidth of 50 MHz. Multiple cross-polarization contacts were used to transfer the polarization from ^1H to ^{13}C CP. The sample was dissolved with 5 mL superheated H_2O and pushed in 6 s to a high-resolution 11.75 T (500 MHz for ^1H) detection spectrometer. After dissolution, the glucose concentration was 30 mM. After waiting for 4 s so that the sample would settle in the NMR tube, sequences of 5° pulses were applied to ^{13}C at time intervals of 1 s, followed by acquisition, either with or without homonuclear ^{13}C decoupling. In both cases, deuterium was decoupled during acquisition. The same experiment was done at thermal equilibrium, by accumulating 128 scans with a 90° excitation pulse.

Acknowledgements

We are indebted to Dr Daniel Abergel for stimulating comments on the pentose phosphate pathway. This work was supported by the Swiss National Science Foundation (SNSF), the Ecole Polytechnique Fédérale de Lausanne (EPFL), the University of Neuchâtel, the Neuchâtel Platform of Analytical Chemistry (NPAC), the Swiss Commission for Technology and Innovation (CTI), and the European Research Council (ERC, contract 'para-water').

References

- 1 E. Miclet, D. Abergel, A. Bornet, J. Milani, S. Jannin and G. Bodenhausen, *J. Phys. Chem. Lett.*, 2014, **5**, 3290.
- 2 W. A. Anderson and R. Freeman, *J. Chem. Phys.*, 1962, **37**, 85.

- 3 J. P. Jesson, P. Meakin and G. Kneissel, *J. Am. Chem. Soc.*, 1973, **95**, 618.
- 4 W. P. Aue, J. Karhan and R. R. Ernst, *J. Chem. Phys.*, 1976, **64**, 4226.
- 5 D. Carnevale, T. F. Segawa and G. Bodenhausen, *Chem. – Eur. J.*, 2012, **18**, 11573.
- 6 T. F. Segawa, D. Carnevale and G. Bodenhausen, *ChemPhysChem*, 2013, **14**, 369.
- 7 A. Hammarström and G. Otting, *J. Am. Chem. Soc.*, 1994, **116**, 8847–8848.
- 8 J. O. Struppe, C. Yang, Y. Wang, R. V. Hernandez, L. M. Shamansky and L. J. Mueller, *J. Magn. Reson.*, 2013, **236**, 89–94.
- 9 J. Ying, F. Li, J. H. Lee and A. Bax, *J. Biomol. NMR*, 2014, **60**, 15–21.
- 10 J. Ying, J. Roche and A. Bax, *J. Magn. Reson.*, 2014, **241**, 97–102.
- 11 L. Castañar, P. Nolis, A. Virgili and T. Parella, *Chem. – Eur. J.*, 2013, **19**, 17283–17286.
- 12 K. Zangger and H. Sterk, *J. Magn. Reson.*, 1997, **124**, 486.
- 13 K. Zangger, *Prog. Nucl. Magn. Reson. Spectrosc.*, 2015, **86–87**, 1–20.
- 14 L. Duma, S. Hediger, B. Brutscher, A. Böckmann and L. Emsley, *J. Am. Chem. Soc.*, 2003, **125**, 11816.
- 15 I. C. Felli and R. Pierattelli, *Prog. Nucl. Magn. Reson. Spectrosc.*, 2015, **84–85**, 1–13.
- 16 J. R. Garbow, D. P. Weitekamp and A. Pines, *Chem. Phys. Lett.*, 1982, **93**(5), 504.
- 17 K. J. Donovan and L. Frydman, *Angew. Chem., Int. Ed.*, 2015, **54**, 594–598.
- 18 M. Tiainen, H. Maaheimo, P. Soininen and R. Laatikainen, *Magn. Reson. Chem.*, 2010, **48**, 117.
- 19 S. P. Colowick and H. M. Kalckar, *J. Biol. Chem.*, 1941, **137**, 789.
- 20 S. P. Colowick and H. M. Kalckar, *J. Biol. Chem.*, 1943, **148**, 117.
- 21 F. Bloch and A. Siegert, *Phys. Rev.*, 1940, **57**, 522.
- 22 L. Emsley and G. Bodenhausen, *Chem. Phys. Lett.*, 1990, **168**, 297.
- 23 K. T. Summanen, *Phys. Lett. A*, 1991, **155**, 335.
- 24 M. Bak, T. Rasmussen and N. Nielsen, *J. Magn. Reson.*, 2000, **147**, 296.
- 25 A. Abragam and M. Goldman, *Rep. Prog. Phys.*, 1978, **41**, 395–467.
- 26 J. H. Ardenkjaer-Larsen, B. Fridlund, A. Gram, G. Hansson, L. Hansson, M. H. Lerche, R. Servin, M. Thaning and K. Golman, *Proc. Natl. Acad. Sci. U. S. A.*, 2003, **100**, 10158–10163.
- 27 A. Bornet, R. Melzi, S. Jannin and G. Bodenhausen, *Appl. Magn. Reson.*, 2012, **43**, 107.
- 28 E. Kupce and R. Freeman, *J. Magn. Reson., Ser. A*, 1993, **102**, 364.
- 29 G. Bodenhausen, R. Freeman and G. A. Morris, *J. Magn. Reson.*, 1976, **23**, 171.
- 30 G. A. Morris and R. Freeman, *J. Magn. Reson.*, 1978, **29**, 433.
- 31 H. Geen, X. L. Wu, P. Xu, J. Friedrich and R. Freeman, *J. Magn. Reson.*, 1989, **81**, 646.
- 32 S. L. Patt, *J. Magn. Reson.*, 1992, **96**, 94.
- 33 A. J. Shaka, J. Keeler, T. Frenkiel and R. Freeman, *J. Magn. Reson.*, 1983, **52**, 335.